



Optical and Microphysical Analysis of Aerosols in Sahelian Zone: Case of the Ouagadougou City in Burkina Faso

Bado Nébon^{1,2}, Mamadou Simina Dramé², Korgo Bruno¹, Kieno P. Florent¹, Saidou Moustapha Sall² and Bathiebo Dieudonné Joseph¹

¹Laboratoire d'Energies Thermiques Renouvelables (LETRE), Université Ouaga I Pr Joseph KI ZERBO, BP 13495 Ouaga, Burkina Faso.

²Laboratoire de Physique de l'Atmosphère et de l'Océan Siméon-Fongang, Université Cheikh Anta DIOP, BP 5085 Dakar-Fann, Sénégal.

ARTICLE INFO

Article history:

Received: 1 May 2018;

Received in revised form:
28 May 2018;

Accepted: 7 June 2018;

Keywords

Aerosol,
AERONET,
HYSPLIT,
Back-Trajectory,
Microphysical and Optical
properties,
Ouagadougou.

ABSTRACT

This paper analyzes aerosols in the Sahelian zone, particularly in Burkina Faso, based on in situ measurements of the AERONET network made from 1999 to 2006. Indeed, we characterize aerosols by studying their optical and microphysical parameters measured on the site of Ouagadougou (12.2° N, 1.4° W). Thus, several types of days were defined based on the daily averages of optical thicknesses observed. Therefore, cases of days with AOT values > 1 and possibly beyond 2.5 or 3 are associated with desert dust occurrences confirmed by the Angstrom coefficient ($\alpha_{440-870} < 0.5$) and the single scattering albedo ($SSA > 0.9$) observed mainly in Winter (DJF) and then in Spring (MAM). These huge falls of mineral dust are due to the proximity of this zone with the Sahel, Burkina Faso being particularly located in the Sahel, as clearly shown by the back-trajectories of the air masses drawn at 300 m, 1.000 m and 3.000 m of altitude. These wind trajectories reveal the presence of desert aerosols in all periods, with an influence in Summer due to distant transport at high altitude, nearly 3.000 m, in thin dust, whereas in Winter and in Spring, dust is generated by low-level winds from the North and Northeast. However, mixed days corresponding to AOT values ≥ 0.5 and $\alpha_{440-870} \geq 0.5$ are dominated by more scattering fine desert particles mixed with too much thin combustion aerosols. The combustion particles are due to transports from the Southern part of the country to the Gulf of Guinea, mainly in Winter, Spring and Autumn.

© 2018 Elixir All rights reserved.

1. Introduction

Burkina Faso is a sub-Sahara African country, specifically located in the Sahel and in the heart of West Africa. Due to its geographical location, the country shares borders with six other states, including Mali and Niger in the Northern part, which are largely affected by the Sahara desert. This position makes Burkina Faso highly exposed to Saharan dust despite anthropogenic emissions related to transport, household activities, agriculture and the density of some of its cities. In West Africa, aerosols are strongly influenced by mineral dust because this zone is close to the Sahara, which is recognized as the largest desert in the world and the first source of dust emissions, with a surface area of nearly 8.5 million km² [1]. Indeed, the main sources of dust in Africa are located on the Northern side, between 18° N and 25° N of latitude and mainly covers the Sahel and the Sahara [2; 3]. At some periods, strong dust storms send out huge quantities of particles into the atmosphere, with the consequence of reducing visibility, modifying the optical characteristics of the atmosphere, as well as radiation on the surface. In addition to this climate impact, dust enormously affects the respiratory system, especially when it is inhaled and then creates serious diseases, notably in children and elderly. Thus, they are responsible for asthma attacks in asthmatic patients, the increase in the number of cardiovascular deaths [4; 5; 6; 7] and a decrease in life

expectancy. Moreover, a study conducted by Sultan et al., 2005 reveals that aerosols are responsible for typical cases of meningitis outbreaks at some precise periods in Africa, notably during the dry season which is strongly influenced by the Harmattan [8]. These dusts are also responsible for a major decrease in atmospheric visibility, road and air traffic jams leading to air disasters and then to the standstill of socio-economic activities [9]. The objective of this research is to contribute to the understanding of the level of pollution due to particles as well as to a better knowledge of aerosols in the West Africa area, mainly in the Sahel. Therefore, we carry out an analysis of the optical and microphysical properties of aerosols in the case of the Ouagadougou City in Burkina Faso and the identification of emission sources, using ground measurements of the AERONET network and the HYSPLIT model.

2. Data and Methodology

2.1. AERONET Inversions (AEROSOL ROBOTIC NETWORK)

The AERONET network is a network of Cimel photometers and solar radiometers installed throughout the world. These radiometers measure the direct and diffuse radiation used by the AERONET inversion code which provides the optical, radiative and microphysical properties of aerosols throughout the atmospheric column for different wavelengths [1]. The inverted optical properties include the optical thickness (AOT), the Angstrom coefficient,

the real and imaginary part of the complex refractive index. Microphysical properties refer to particle size distribution and the sphericity rate. As for the radiative properties, they are shown by the single scattering albedo, the phase function, the asymmetry parameter, the spectral flow, the radiative forcing and the efficiency of the radiative forcing. The developments of the AERONET inversion codes are described by [10; 11; 12; 13]. All inverted parameters are available on the AERONET network site, in daily, monthly, annual average values and even in instantaneous values [14]. The optical thickness which reflects the mitigation of the radiation by the aerosol-loaded atmosphere layer is obtained by direct measurement in 4 spectral bands (440, 670, 870, 1.020 nm). This is a key indicator, as is the visibility of atmospheric transparency. Thus, for this study, we use parameters such as the optical thickness (AOT), the single scattering albedo (SSA), the Angstrom coefficient and the volume distribution obtained by AERONET inversion.

2.2. HYSPLIT Model (HYbrid Single-Particle Lagrangian Integrated Trajectory)

There are two approaches to simulating air masses movement in time and space: the Eulerian model and the Lagrangian model [15]. Indeed, the Eulerian model considers fixed points of space through which the air masses circulate, whereas the Lagrangian model is based on the temporal spatial movements of air parcel [16]. The HYSPLIT model, as its name suggests, is a hybrid between both approaches (Eulerian and Lagrangian). The Lagrangian approach takes into account the advection and diffusion phenomena and then allows the calculation of the air masses concentrations by considering a system of fixed meshes [17]. Thus, the Lagrangian model is more suitable for calculating trajectories under conditions of instability, unlike the Eulerian model, notably when it comes to predicting the dispersion and transport of particles under these conditions [18]. The trajectory model provides a description of the position X of the air parcel at the time t , as a function of time and its position X_0 at the time t_0

follows:

$$X(t) = X(X_0, t) \quad (1)$$

All positions $X(t)$ describe the front trajectories of the point X_0 . The coordinates of this point at the initial time are called the Lagrangian coordinates [16]. The inverse transform gives the expression of $X_0(t)$ according to the function $X(t)$ and time t according to the following relation (2) which enables to describe the retro-trajectories.

$$X_0(t_0) = X_0(X, t) \quad (2)$$

The function $X(X_0, t)$ is a trajectory solution defined by the equation below:

$$\frac{dX}{dt} = V(x, t) \quad (3)$$

$V(x, t)$ is the wind speed vector at the time t .

The analytical solution of the trajectory equation can be obtained by using the finite difference approximation [19] which gives the development of $X(t)$ as a Taylor series at the time $t_1 = t_0 + \Delta t$ where $t = t_0$. We then get:

$$X(t_1) = X(t_0) + (\Delta t) \frac{dX}{dt} \Big|_{t_0} + \frac{1}{2} (\Delta t)^2 \frac{d^2 X}{dt^2} \Big|_{t_0} + \dots \quad (4)$$

The first approximation of this equation for zero acceleration, gives a simple solution:

$$X(t_1) \approx X(t_0) + (\Delta t) \dot{X}(t_0) \quad (5)$$

The development of X in Taylor series at $t_1 = t_0 + \Delta t$ gives:

$$X(t_0) = X(t_1) - (\Delta t) \frac{dX}{dt} \Big|_{t_1} + \frac{1}{2} (\Delta t)^2 \frac{d^2 X}{dt^2} \Big|_{t_1} - \dots \quad (6)$$

A combination of the two developments (4) and (6) gives the following expression of $X(t_1)$:

$$X(t_1) = X(t_0) + \frac{1}{2} (\Delta t) [\dot{X}(t_0) + \dot{X}(t_1)] + \frac{1}{4} (\Delta t)^2 \left[\frac{d\dot{X}}{dt} \Big|_{t_0} - \frac{d\dot{X}}{dt} \Big|_{t_1} \right] + \dots \quad (7)$$

The first approximation of the solution when the acceleration is zero is:

$$X(t_1) \approx X(t_0) + \frac{1}{2} (\Delta t) [\dot{X}(t_0) + \dot{X}(t_1)] \quad (8)$$

This solution corresponds exactly to that described by Draxler (1998) in the modeling system of HISPLYT_4 for the trajectory, the dispersion and the deposit which is as follows:

$$P(t + \Delta t) = P(t) + 0.5[V(P, t) + V(P', t + \Delta t)]\Delta t \quad (9)$$

In this expression, $P(t)$ is the three-dimensional position at the time of reference t , $P(t + \Delta t)$ at the time $t + \Delta t$, $V(P, t)$ and $V(P', t + \Delta t)$ wind speed vectors of the wind at times t and $t + \Delta t$ respectively. In this paper, the model HYSPLIT served as a tool for calculating the retro-trajectory of air masses, which enables to show the nature and origin of the particles observed above Ouagadougou.

3. Results and analysis

Measurements based on the properties of aerosols in Burkina Faso, particularly in the site of Ouagadougou (12.2° N, 1.4° W), range from April 30, 1999 to January 11, 2007, representing the end of operation of the photometer installed on this site. The end of photometric measurements since this period coupled with the lack of in situ measuring tools constitute a major difficulty for a current characterization of aerosols in this area, notably in recent years. Thus, for our study, the available AERONET measurements are from April 30, 1999 to December 31, 2006. These are level 2 data, which quality is automatically assured, processed by eliminating contaminations dues to clouds and then manually checked. These are inversions of the version 2 of the " Direct Sun Algorithm " [20].

3.1. Inter-annual variation of the daily averages of optical thickness

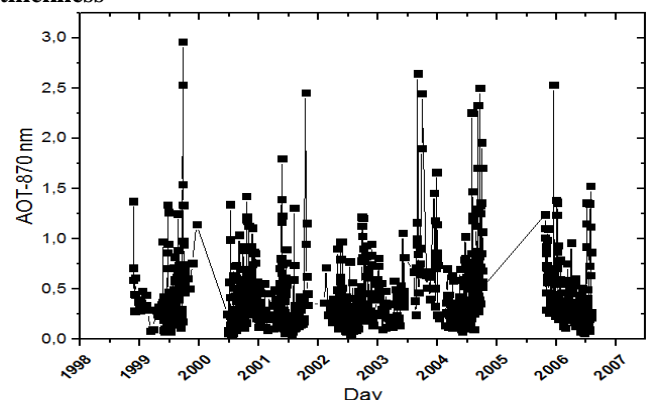


Figure 1. Daily average of optical thickness (AOT) measured at 870 nm on the Site of Ouagadougou.

The daily optical thicknesses included are measured from 1999 to 2006 in a wavelength of 870 nm and are represented in figure 1. Several peaks are observed according to AOT values. These peaks give the nature of the atmosphere and make it possible to define the various events in the Sahel and the Sahara or local emissions following the socio-economic activities in the Ouagadougou City. Thus, peaks of high AOT values higher than 1 and above 2.5 are encountered in all the years and mostly occur between January and June. In addition, the intensity of these peaks shows the degree of the impact of desert dusts on this city due to its closeness to the Sahara, which remains the largest source of dust in the world according to several heights [2; 21; 22]. As for the secondary peaks of AOT less than 1, they show a less loaded atmosphere due to mix days characterized by a mixture of mineral aerosols and combustion products. In addition, these days are often associated with a dominance of thin aerosols, notably made of thin particles of mineral dust. With AOT days less than 0.5, they are characterized by medium, year-round, clear aerosol conditions in which aerosol particles seem negligible [23].

3.2. Inter-annual variation of the daily averages of Angstrom parameter

The Angstrom coefficient is an indicator of particle size. This gives an idea on their origin and their formation pattern. Figure 2 shows the aerosol pattern according to the days marked by the AOT values. For the series of measurements considered, Angstrom values are contained in the spectral

range of 440-870 nm covering the measurement wavelength of the AOT (Figure 1). Its analysis reveals the presence of the two main classes of particles in the Ouagadougou site, including thin particles associated with $\alpha_{440-870} > 0.5$ and coarse particles corresponding to $\alpha_{440-870} < 0.5$ [20; 24]. The study of this parameter according to the particle load of the atmosphere shows that, whatever the season, days with AOT values < 1 are characterized by an aerosol suspension influenced by thin and large particles. Therefore, it can be noticed that days with large particles, mainly composed of mineral aerosols that dominate the particles, are numerous. However, days with $\text{AOT} > 1$ are mainly influenced by essentially large dust particles ($\alpha_{440-870} < 0.5$). In addition, periods in Winter (DJF) and Spring (MAM) correspond to those dusty periods when AOT values ≥ 2 and up to 3 (AOT = 3). It should also be noted that days with Angstrom values ≥ 0.5 are much encountered in Winter (DJF), Autumn (SON) and then in Summer (JJA) while MAM reveals to be more under the influence of desert dust, corresponding to Angstrom values $\alpha_{440-870} < 0.5$. Indeed, mineral aerosols are most often related to distant transport from the main emission sources located in the North of the continent [2], source of the dust periods associated with peaks of $\text{AOT} \geq 2$ observed mainly in Winter and Spring. However, the thin pattern observed for days with less loaded atmosphere ($\text{AOT} < 1$) shows the state of mixing of the aerosol population consisting of thin particles from probably local anthropogenic emissions and thin desert particles.

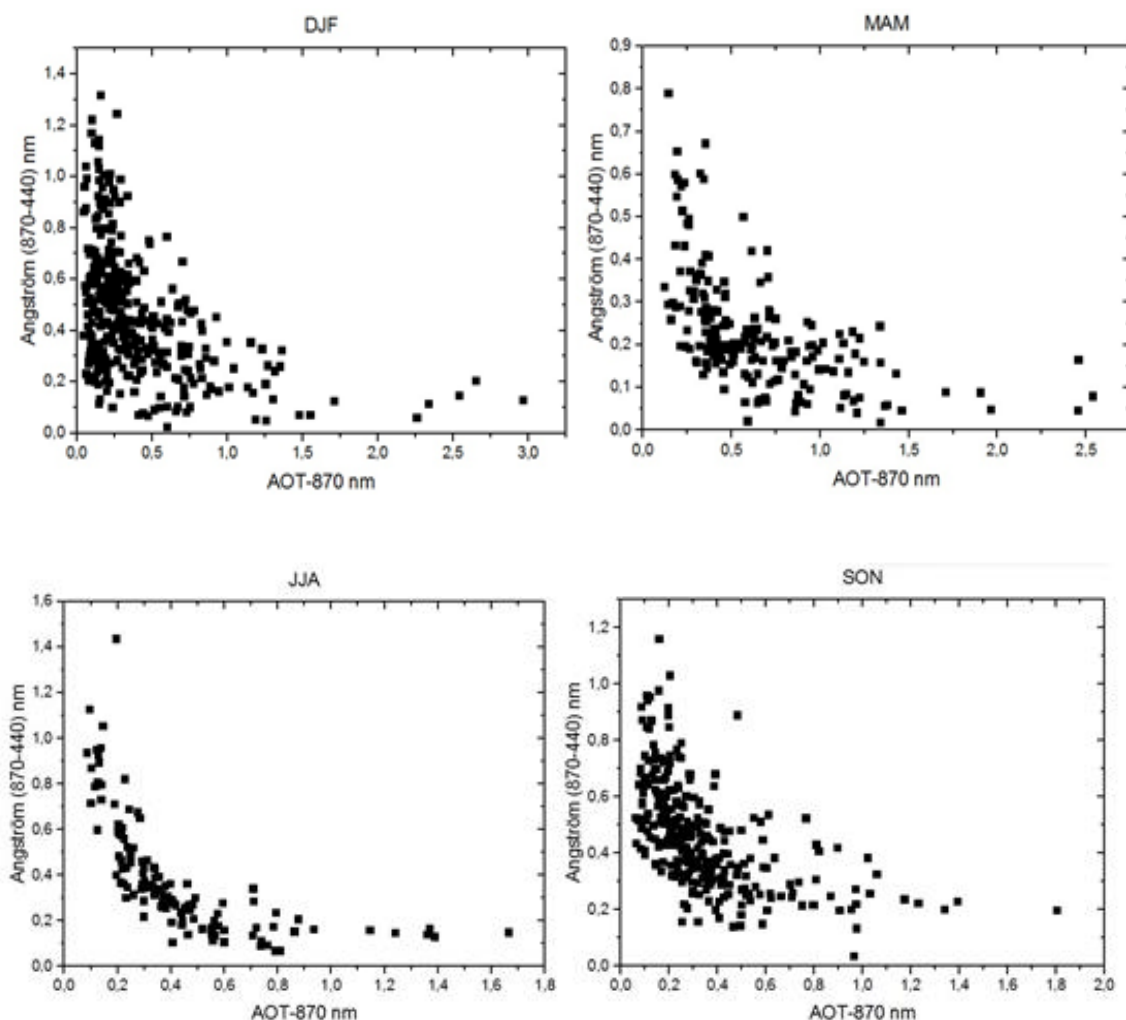


Figure 2. Daily averages of the Angstrom parameter ($\alpha_{440-870}$) measured in the spectral range of 440-870 nm according to the AOT at 870 nm in the Ouagadougou site.

3.3. Inter-annual variation of daily averages of single scattering albedo

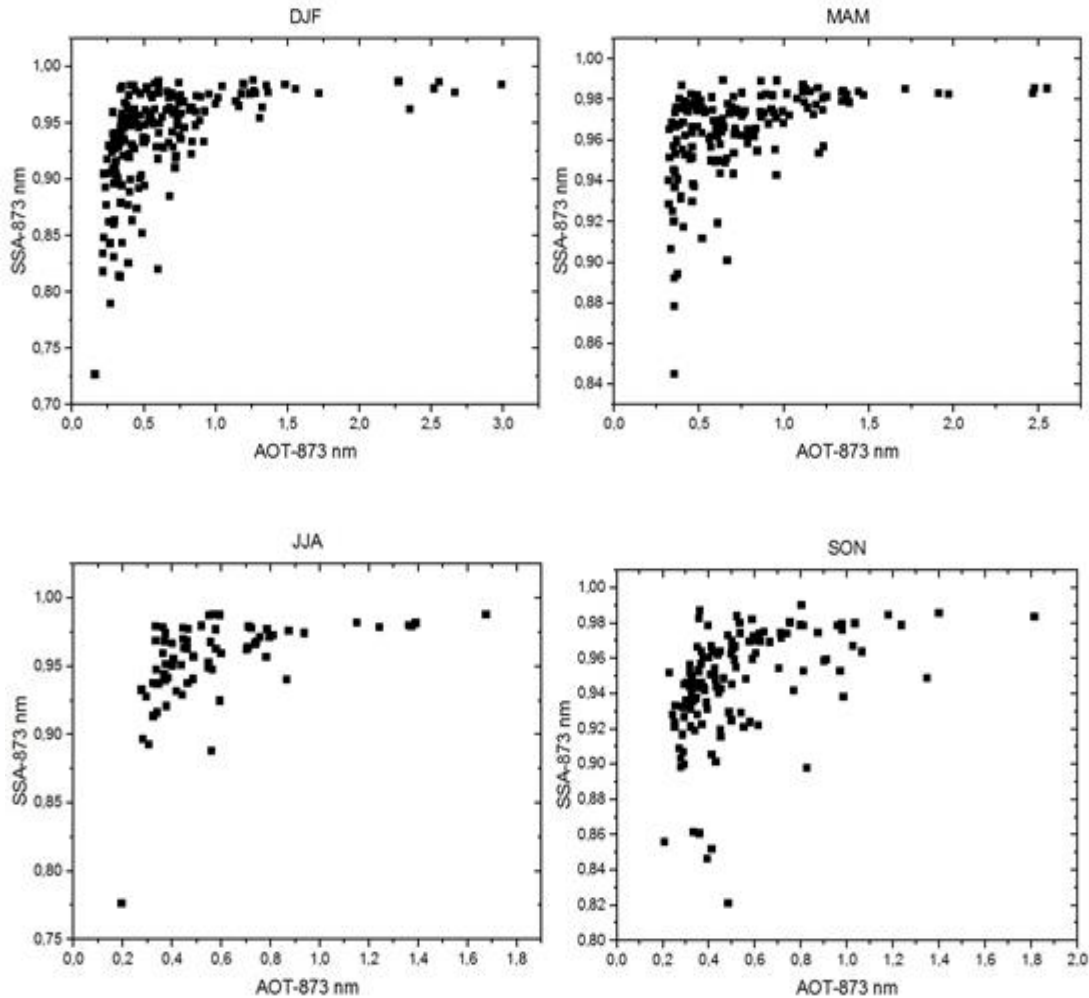


Figure 3. Daily average of single scattering albedo (SSA) measured at 873 nm according to the AOT at 873 nm in the Ouagadougou site.

Single scattering albedo (SSA) analysis shows the dominance of particle scattering in all seasons with a majority of days defined by SSA values > 0.9 (Figure 3). This is specific to desert aerosols and shows the natural origin of the particles due to the mechanical wind action, confirming the high level of dusts with a low content of mainly absorbing combustion aerosols. These carbonaceous particles are more seen in days with values of SSA < 0.9 , which are much more noticed in Winter (DJF). These days correspond to the values of AOT < 1 . But days with AOT > 1 exclude any presence of absorbing aerosols, thus showing the prevailing impact of dust in these days. This explains dusts falls noticed in December-January- February (DJF) then in March-April-but (MAM).

3.4. Air mass trajectories and particles origins

HYSPLIT retro-trajectory analysis makes it possible to highlight the origin of particles and confirms their nature as revealed by Angstrom parameter ($\alpha_{440-870}$) and the single scattering albedo (SSA). The trajectories are drawn at 300 m, 1,000 m and 3,000 m altitude and refer to the atmospheric low layer strongly influenced by aerosols. Therefore, it should be noted that at 3,000 m of altitude, the transport of particles concerns the thin ones which are a mixture of combustion aerosols and thin desert particles whereas large particles are rather seen at an altitude of nearly 1,000 m and 2,000m [23]. The trajectories are calculated at a time step of 6 hours for 96 hours, i.e. 4 days.

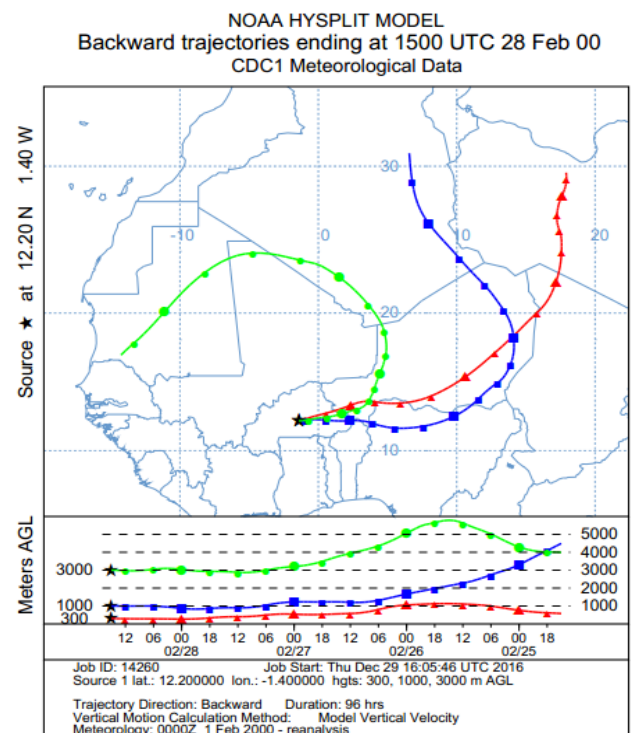


Figure 4.1

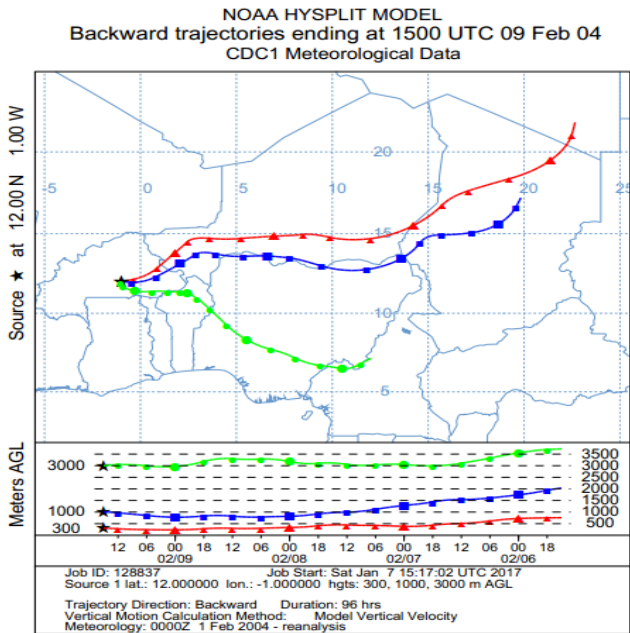


Figure 4.2

NOAA HYSPLIT MODEL
Backward trajectories ending at 1400 UTC 26 Mar 01
CDC1 Meteorological Data

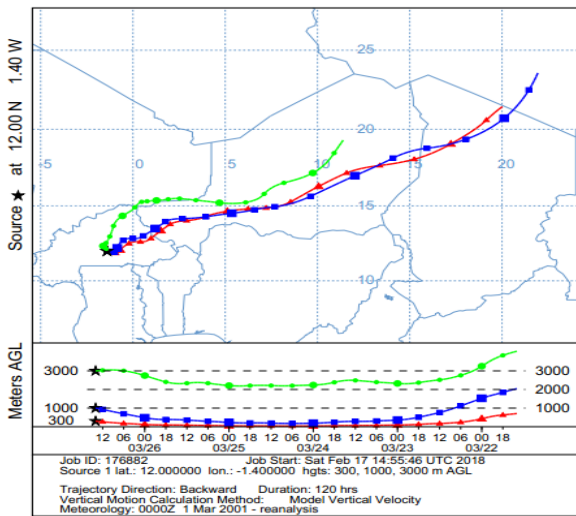


Figure 4.3

NOAA HYSPLIT MODEL
Backward trajectories ending at 1600 UTC 06 Mar 04
CDC1 Meteorological Data

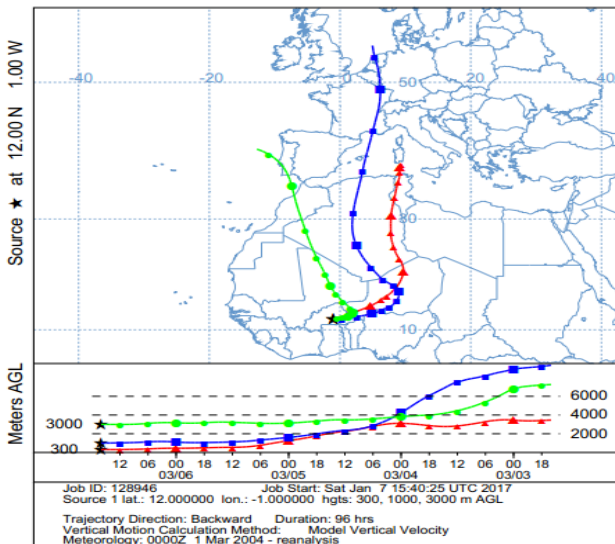


figure 4.4

NOAA HYSPLIT MODEL
Backward trajectories ending at 1600 UTC 07 Mar 05
CDC1 Meteorological Data

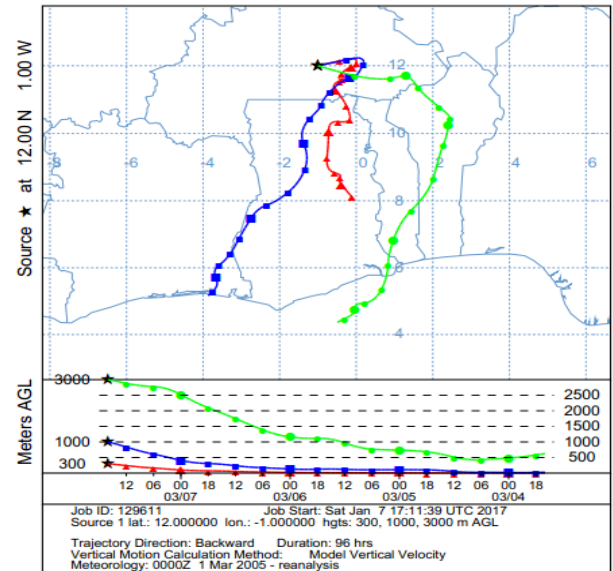


Figure 4.5

NOAA HYSPLIT MODEL
Backward trajectories ending at 0900 UTC 25 May 06
CDC1 Meteorological Data

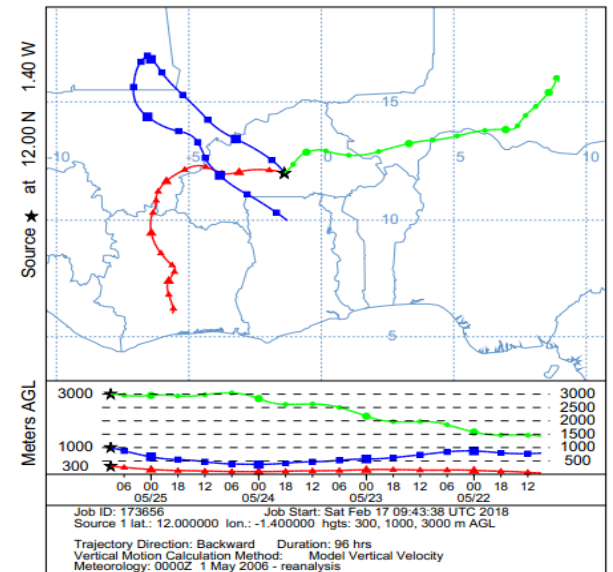


Figure 4.6

NOAA HYSPLIT MODEL
Backward trajectories ending at 0900 UTC 06 Jun 04
CDC1 Meteorological Data

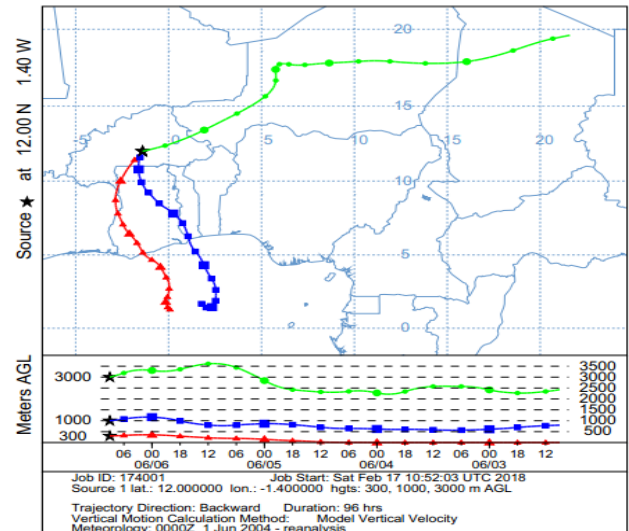


Figure 4.7

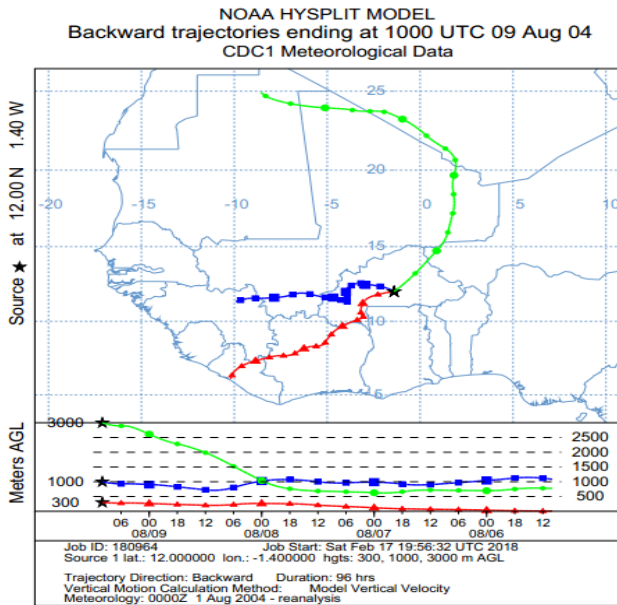


Figure 4.8

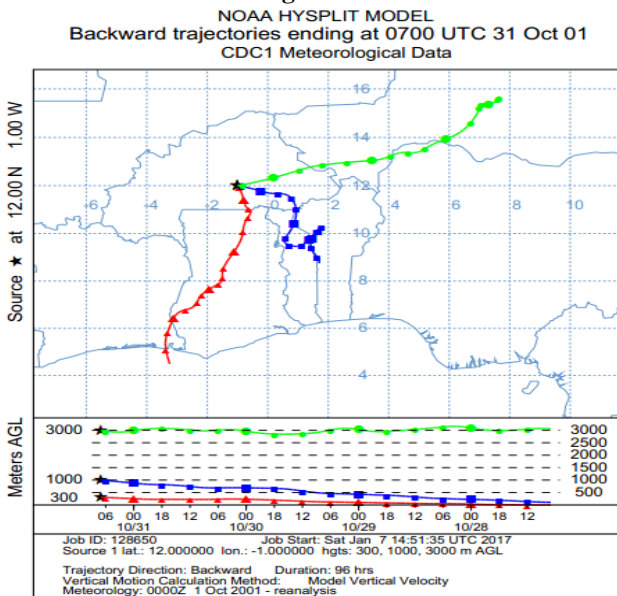


Figure 4.9

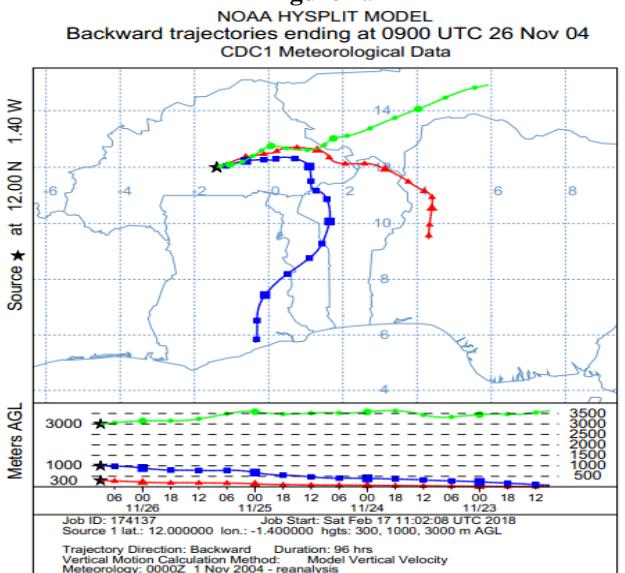


Figure 4.10

Figure 4. Air mass trajectories drawn using HYSPLIT model at 300 m (in red), 1,000 m (in blue) and 3,000 m (in green).

In Winter (DJF), particles are strongly dominated by dust due to the arrival of the air masses from the North and North-East (Figures 4.1 and 4.2). This meridional wind blow shows the impact of the sources of emission hosted in the Sahara, notably the North-West of Mali, the South of Algeria, the Libyan desert (figure 4.1) and the Bodélé depression in Chad (figure 4.2). Thus, retro-trajectories show quite well the primary nature of aerosols coming from the Sahara, accounting for the peaks of $AOT \geq 2$ (Figure 1) and Winter dust events related to low-level winds observed at an altitude of 300 m (red curve) and 1.000 m (blue curve). In addition, the presence of combustion particles in Winter is due to the high-altitude transport towards the Gulf of Guinea, shown by the trajectories at 3.000 m (Figure 4.2). In Spring (MAM), the effect of mineral dust is also noticed with the arrival of air masses from the East (Figure 4.3) and the North (Figure 4.4). Indeed, the Spring is marked by a mixture of mineral aerosols from the Sahara and combustion particles carried by winds from the South and South-West (figures 4.5 and 4.6), notably due to the combustion in the Gulf of Guinea. These winds are due to the strong sunshine and the transition period between the Harmattan flow and the Monsoon. Summer (JJA) in the Sahel is strongly dominated by the Monsoon flow; hence the origin of the air masses towards the South and the South-West (figure 4.7 and 4.8) due to the convection in this Winter period. The arrival of the maritime trade winds is clearly visible by the air masses at an altitude of 300 m and 1,000 m (Figures 4.7 and 4.8). Yet, the effect of dust in Summer is mainly due to the distant transport of aerosols in the Saharan air layer shown by the trajectories at 3,000 m (green curve) of altitude. In Autumn (SON), winds come from the South and South-East carrying products of combustion in the Gulf of Guinea between 300 and 1,000 m of altitude (figure 4.9 and 4.10). These particles are then mixed with the thin desert particles transported by wins from the East at high altitude shown by the trajectories at 3,000 m. In addition, Autumn in West Africa corresponds to the transition between the Monsoon and the Harmattan. This withdrawal of the Monsoon is through the displacement of the ITCZ which is around 10° N of latitude, accounting therefore for the trade winds of South and South-East in this period of Autumn [25].

3.5. Daily particle size distribution

The volume size distribution characterizes the aerosol pattern observed on the site and enables to see the evolution of the class of particles according to the particle load of the atmospheric layer. Indeed, the volume distribution of the aerosols is measured in 22 modal radii contained in a range of radii ranging from 0.05 to 15 μ m. This image (Figure 5) confirms the dominant impact of large particles that are sources of dust periods with characterized by days with values of $AOT > 1$ and Angstrom coefficient $\alpha_{440-870} < 0.5$. Most of these particles have a size between 1 μ m and 10 μ m and dominate the volume distribution because of their large size (Figure 5a and 5b). However, the importance of pollution particles smaller than 1 μ m is clearly observed during days when $AOT < 1$, referred to as mixed days and characterized by $AOT \geq 0.15$ and $\alpha_{440-870} \geq 0.4$ [23]. These days reveal the mixing state of the aerosols because of the peaks observed around $r = 0.1 \mu$ m and $r = 2$ to 3 μ m (Figure 5c). But a strong domination of the thin pattern of the mineral dust particles can be noticed when Angstrom coefficient values are higher than 0.5.

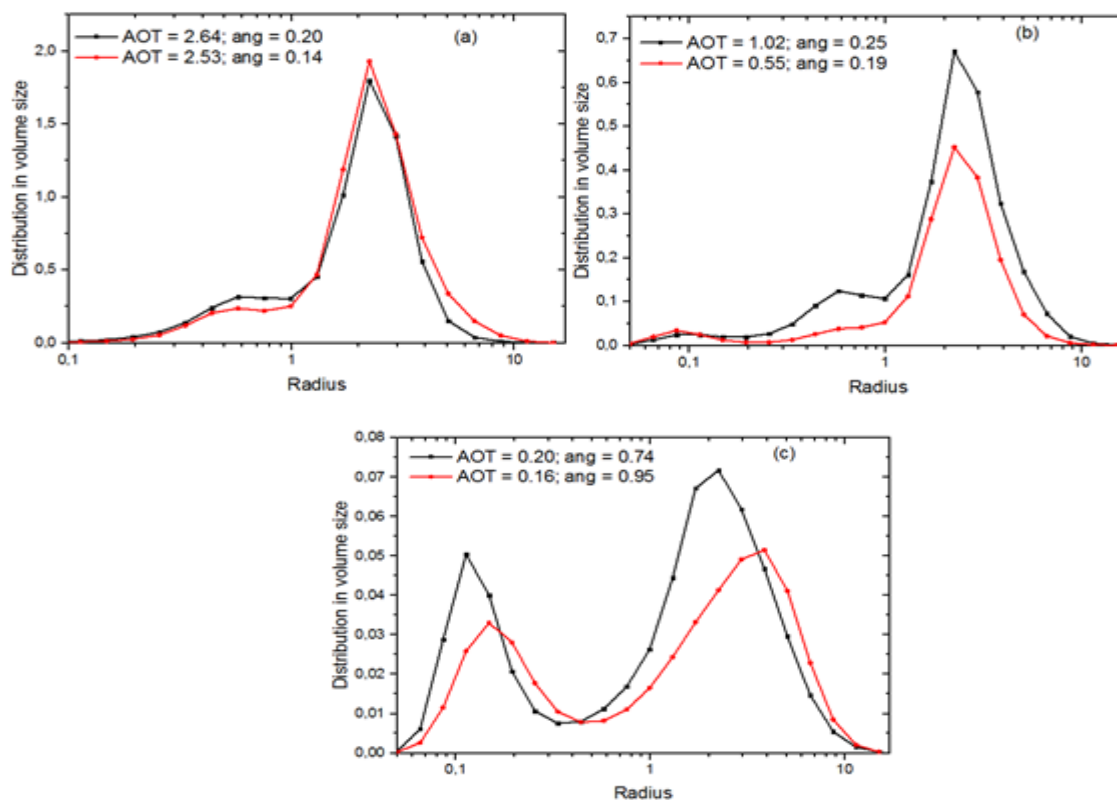


Figure 5: Distribution in volume size ($\mu\text{m}^3/\mu\text{m}^2$) according to modal radius (μm). Days are defined by the optical thickness (AOT) and the Angstrom coefficient (ang).

4. Conclusion

A characterization of aerosols is made based on photometric measurements of the AERONET network in Ouagadougou. This enabled to highlight the types and the state of mixing of the particles observed in Ouagadougou, Burkina Faso. However, the aerosols observed on this site are strongly dominated by mineral dusts because of their scattering character marked by $\text{SSA} \geq 0.9$, corroborated by the volume distribution and the trajectories of the air masses. This state of aerosol mixing defined several days after AOT and particle size, with a particularity for some days characterized by $\text{AOT} \geq 2$. These days are associated with a very considerable scattering of aerosols also known as dust fall-outs. In addition, the trajectories of air masses confirm the intensity of dust coming from the Sahara, notably in Winter and Spring. This should be added the combustion products from the Gulf of Guinea conveyed by the South and South-East winds in Autumn.

Bibliography

[1] B. Korgo, J. . Roger, and J. Bathiebo, "Climatology of air mass trajectories and aerosol optical thickness over Ouagadougou," *Glob. J. Pure Applied Sci.*, vol. 19, pp. 169–181, 2013.

[2] J. M. Prospero, P. Ginoux, O. Torres, S. E. Nicholson, and T. E. Gill, "Environmental characterization of global sources of atmospheric soil dust identified with the nimbus 7 total ozone mapping spectrometer (TOMS) absorbing aerosol product," *Rev. Geophys.*, vol. 40, no. February, pp. 1–31, 2002.

[3] S. Engelstaedter, I. Tegen, and R. Washington, "North African dust emissions and transport," *Sci. Direct*, vol. 79, pp. 73–100, 2006.

[4] R. J. Delfino, C. Sioutas, and S. Malik, "Review Potential Role of Ultrafine Particles in Associations between Airborne Particle Mass and Cardiovascular Health," *Environ. Health Perspect.*, vol. 113, no. 8, pp. 934–946, 2005.

[5] K. Donaldson, V. Stone, A. Seaton, and W. Macnee, "Ambient Particle Inhalation and the Cardiovascular System : Potential Mechanisms," *Environ. Health Perspect.*, vol. 109, no. 4, pp. 523–527, 2001.

[6] D. Liao, J. Creason, C. Shy, R. Williams, R. Watts, and R. Zweidinger, "Daily Variation of Particulate Air Pollution and Poor Cardiac Autonomic Control in the Elderly," *Environ. Health Perspect.*, vol. 107, no. 7, pp. 521–525, 1999.

[7] J. M. Prospero, E. Blades, R. Naidu, G. Mathison, H. Thani, and M. C. Lavoie, "Relationship between African dust carried in the Atlantic trade winds and surges in pediatric asthma attendances in the Caribbean," 2008.

[8] B. Sultan, K. Labadi, J.-F. Guégan, and S. Janicot, "Climate Drives the Meningitis Epidemics Onset in West Africa," *Plos Med.*, vol. 2, no. 1, pp. 0043–0049, 2005.

[9] R. Greeley, D. G. Blumberg, J. F. Mchone, A. Dobrovolskis, J. D. Iversen, N. Lancaster, K. R. Rasmussen, S. D. Wall, and B. R. White, "Applications of spaceborne radar laboratory data to the study of aeolian processes," *Geophys. Res.*, vol. 102, no. 97, pp. 10971–10983, 1997.

[10] O. Dubovik and D. King, "A flexible inversion algorithm for retrieval of aerosol optical properties from Sun and sky radiance measurements," *J. Geophys. Res.*, vol. 105, 2000.

[11] O. Dubovik, B. N. Holben, T. Lapyonok, A. Sinyuk, M. I. Mishchenko, P. Yang, and I. Slutsker, "Non-spherical aerosol retrieval method employing light scattering by spheroids," *Geophys. Res. Lett.*, vol. 29, no. 10, pp. 3–6, 2002.

[12] O. Dubovik, "Optimization of numerical inversion in photopolarimetric remote sensing," *Kluwer Acad. Publ. Print. Netherlands*, pp. 65–106, 2004.

[13] O. Dubovik, A. Smirnov, B. N. Holben, M. D. King, Y. J. Kaufman, T. F. Eck, and I. Slutsker, "Accuracy assessments of aerosol optical properties retrieved from Aerosol Robotic Network (AERONET) Sun and sky," *Geophys. Res.*, vol. 105, no. D8, pp. 9791–9806, 2000.

- [14]M. Drame, B. O. Bilal, M. Camara, V. Sambou, and A. Gaye, "Impacts of aerosols on available solar energy at Mbour , Senegal," *J. Renew. Sustain. Energy*, vol. 4, pp. 1–13, 2012.
- [15]J. C. Carvalho, M. T. Vilhena, and D. M. Moreira, "Comparison between Eulerian and Lagrangian semi-analytical models to simulate the pollutant dispersion in the PBL," *Appl. Math. Model.*, vol. 31, pp. 120–129, 2007.
- [16]A. Stohl, "Computation , accuracy and applications of trajectories — a review and bibliography," *Atmos. Environ.*, vol. 32, no. 6, pp. 947–966, 1998.
- [17]R. R. Draxler, "An Overview of the HYSPLIT _ 4 Modelling System for Trajectories , Dispersion , and Deposition," *Aust. Meteorol. Mag.*, vol. 47, pp. 295–308, 1998.
- [18]Z. Zhang and Q. Chen, "Comparison of the Eulerian and Lagrangian methods for predicting particle transport in enclosed spaces," *Atmos. Environ.*, vol. 41, no. 25, pp. 5236–5248, 2007.
- [19]J. L. Walmsley and J. Mailhot, "Atmosphere-Ocean On the numerical accuracy of trajectory models for long - range transport of atmospheric pollutants," *Atmosphere-Ocean*, vol. 21, pp. 14–39, 1983.
- [20]C. Diarra and A. BA, "Analysis of optical parameters of atmospheric aerosols, their distribution and their scattering albedo by photometric measurements in Mali," *Afrique Sci.*, vol. 10, no. 2, pp. 82–97, 2014.
- [21]B. Laurent, B. Marticorena, G. Bergametti, and J. F. Le, "Modeling mineral dust emissions from the Sahara desert using new surface properties and soil database," *J. Geophys. Res.*, vol. 113, no. D14218, pp. 1–20, 2008.
- [22]E. T. N. Datchoh, I. Diallo, S. S. Konaré, K. O. Ogunjobi, A. Diedhiou, and M. Doumbia, "Dust induced changes on the West African summer monsoon features," *Int. J. Climatol.*, pp. 2–15, 2017.
- [23]M. S. Drame, X. Ceamanos, J. L. Roujean, A. Boone, J. P. Lafore, D. Carrer, and O. Geoffroy, "On the Importance of Aerosol Composition for Estimating Incoming Solar Radiation: Focus on the Western African Stations of Dakar and Niamey during the Dry Season," *Atmosphere (Basel)*, vol. 6, pp. 1608–1632, 2015.
- [24]K. O. Ogunjobi, Z. He, and C. Simmer, "Spectral aerosol optical properties from AERONET Sun-photometric measurements over West Africa," *Atmos. Res.*, vol. 88, pp. 89–107, 2008.
- [25]M. S. Drame, "Characterization and climate impacts of aerosols in West Africa," Doctorate Thesis, University Cheick Anta DIOP of Dakar, 2012.